



ANALYZING FORMABILITY AND SURFACE QUALITY OF CU-AL BIMETALLIC SHEETS WITH SINGLE POINT INCREMENTAL FORMING TECHNIQUE

Ankitkumar C. Pambhar, Research scholar, Gujarat Technological University, Ahmedabad, Gujarat.

Dr. Janak B. Valaki, Government Engineering College, Bhavnagar; Gujarat Technological University, Ahmedabad, India

Abstract

The Single Point Incremental Forming (SPIF) technique is recognized for its cost-effectiveness and versatility in manufacturing intricate components, distinguishing it from conventional methods. The study explores the SPIF operational variables and their influence on the formability, minimum thickness, and surface quality of Cu-Al bimetallic sheets. Experimental parameters include step depth, forming speed, spindle rotation, and layer configuration. Results indicate that step depths between 0.2mm to 1.0 mm enhance forming depth, while forming speeds of 250 mm/min to 1250 mm/min improve thickness variation. Spindle speeds ranging from 500 rpm to 2500 rpm enhance surface finish. The Cu-Al layer configuration exhibits higher maximum forming wall angles compared to Al-Cu arrangements. These findings provide insights into optimizing SPIF parameters for Cu-Al bimetallic sheets, contributing to their efficient manufacturing.

Keywords: Single point incremental forming, Cu-Al bi-metallic composite sheet, Formability, Surface quality.

I. Introduction

The single point incremental forming (SPIF) technique is renowned in the industry for its cost-effectiveness in manufacturing intricate and specialized components within a short timeframe and low volume. This sets SPIF apart from conventional sheet metal forming methods [1]. In order to attain the intended shape utilizing a CNC machine, SPIF utilizes a round nose tool to selectively deform the metal sheet along a predetermined tool path [2]. Evaluations of the SPIF procedure illuminate its manifold advantages and benefits, underscoring its adaptability across a spectrum of sectors and processes. This adaptability not only enhances its utility but also positions SPIF as a pivotal procedure in shaping the future landscape of the industry. The ability of SPIF to seamlessly integrate into diverse applications suggests a promising trajectory for its widespread adoption and influence in manufacturing practices [3][4].

In assessing successful SPIF component formation, crucial performance indicators include maximum forming wall angle and thickness variation. Research findings indicate that in square pyramid formations, fractures occur primarily in the corner section due to heightened deformation compared to straight surfaces [5]. In their study, H. Arfa et al. examined how process parameters affect formability and thickness distribution using Al 3003-O sheet material. Their study revealed non-uniform thinning during the formation of cone geometries and concentrated thinning at corner areas in pyramid geometries [6]. Forming speed in the Single Point Incremental Sheet Forming (SPIF) process significantly influences forming time, thereby affecting energy consumption levels. An enhancement in formability was observed as forming speed decreased, accompanied by a proportional increase in forming time [7]. The impact of forming speed and step depth on formability and surface quality are significant considerations in the Incremental Sheet Forming (ISF) process. Forming speed directly impacts the time taken for forming, thereby influencing energy consumption and potentially formability. Similarly, step depth, which defines the distance between successive tool tracks, plays a crucial role in determining surface quality and formability. Both parameters interact with each other and with other process variables, necessitating thorough investigation to optimize outcomes. Additionally, variations in these parameters can affect the overall performance and quality of the formed components [8]. Nonetheless, researchers have noted

that as step-depth increases, the formability of metals tends to decrease, or it may have a minimal impact on it [9]. The incremental forming operation can be conducted with or without spinning the forming tool [10]. Establishing pure rolling conditions is crucial to minimize friction levels, achieved by selecting appropriate spindle speed and feed for the chosen tool diameter [11]. Studies have indicated that formability tends to improve with higher rotational speeds [12][13].

Forming flaws, particularly sheet thinning, have long impeded the widespread adoption of the process. A study on multiple passes of forming suggests that an expansion in the overall plastic deformation zone leads to enhanced thickness uniformity during the process [14]. Moreover, incremental forming of DC04 sheet indicates that employing a conventional tool trajectory results in a strong correlation between minimum thickness and tool diameter, while the region of minimum thickness is significantly influenced by step depth [15]. The interaction between the tool and sheet blank also affects surface irregularity. Research on forming AA7075T0 sheet demonstrates that, compared to a non-spinning tool, a rotating forming tool yields superior surface quality [16]. Additionally, regarding Al 5052, the surface roughness initially increases with incremental depth up to a certain angle, followed by a reduction during incremental forming [17].

Several studies have investigated the shaping of composite metals and the related operational parameters [18][19]. However, incremental bimetallic sheet forming remains an area with limited research. This present experimental inquiry aims to investigate the impact of step depth, forming speed, and spindle rotation on formability, minimum thickness, and surface roughness.

II. Materials and Methods

2.1 Material

In the present experimental study, bimetallic composite sheets comprising Cu and Al with a combined thickness of 1 mm were employed. These sheets consisted of a 0.2 mm thick layer of Copper 11000 and a 0.8 mm thick layer of Aluminum 1060. The dimensions of the samples utilized in the experiments were 150 mm x 150 mm x 1 mm. The experiments were conducted on both the Aluminum side, and the conformation experiment was performed on the Al side and Cu side respectively.

Table.1 : Cu-Al composite sheet chemical composition (%wt).

Aluminum	Ele.	Si	Fe	Cu	Mn	Zn	Ti	Ni	Zr	Al
1060 alloy	%wt	0.056	0.22	0.002	0.001	0.001	0.011	0.003	0.001	Balance
Copper	Ele.	Si	Fe	Pb	Mn	Zn	Bi	Ni	Sb	Cu
11000	%wt	0.007	0.01	0.017	0.001	0.082	0.003	0.014	0.004	Balance

2.2 Experimental Setup

Figure 1 illustrates the setup configuration and the methodology employed for securing a Cu-Al composite sheet within the setup. A hemispherical-headed tool crafted from tungsten carbide was firmly fixed in the spindle. The bimetallic sheet was securely held between clamping plates to eliminate any potential movement of the sheet blank. Subsequently, the setup was affixed onto a CNC milling center for the experimental procedures. The interaction between the forming tool and the Cu layer during the forming process is denoted as the Cu-Al layer arrangement, and vice versa for the Al layer.

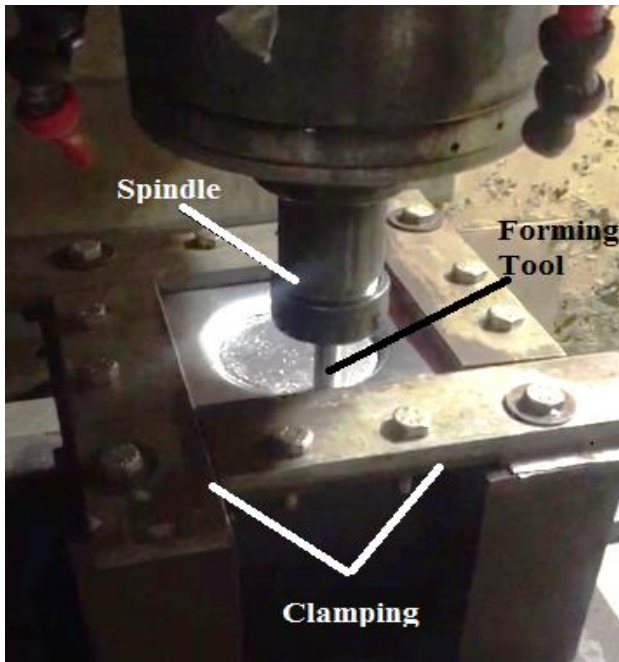


Figure 1: Set-up mounted on the machine.

2.3 Experimental conditions and response evaluation

The current experimental endeavour centered on achieving successful forming of the bimetallic sheet. Various process parameters, such as step depth, forming speed, spindle speed, and layer arrangement, were considered for the experiments. The ranges of these process parameters, along with the response parameters, were detailed in Table 2. To ascertain the maximum forming wall angle for the present experimental study, a truncated cone type geometry with variable generatrix was employed. Figure 2 illustrates the truncated cone geometry utilized in the study.

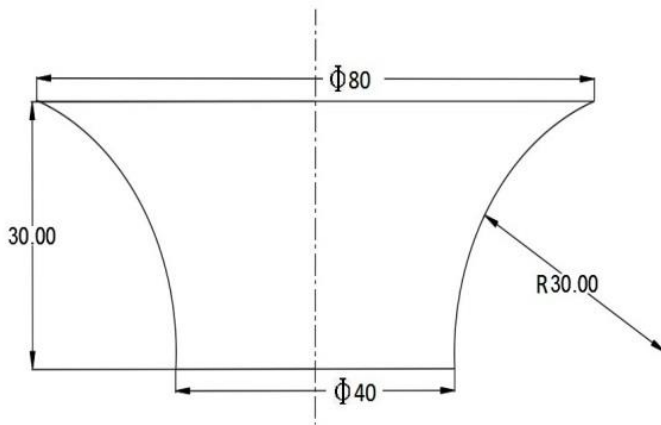


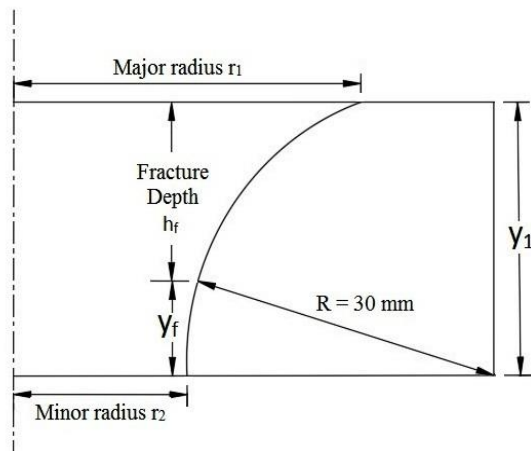
Figure 2: Truncated cone geometry for SPIF

In assessing the maximum angle for wall formation of the formed samples, Vernier height gauges were employed to ascertain the forming depth until fracture occurs (h_f). Figure 3(a) provides an illustration of the terminology associated with the geometry of the generated truncated cone. The truncated cone geometry constructed follows this geometric relation:

$$\text{Maximum forming angle} = \Psi_{max} = \cos^{-1} \left(\frac{y_f}{R} \right) = \cos^{-1} \left(\frac{y_1 - h_f}{R} \right)$$

The maximum angle for wall formation was determined utilizing the previously mentioned equation. In order to assess the formability of the material, it was essential to analyze the strain distribution. This analysis was conducted using a circle grid technique to scrutinize the strain distribution across the material. Before deformation, a circular grid with a circle diameter of 5 mm was screen printed

onto the sheet. Subsequently, strain measurements were performed utilizing a 3D microscope, as shown in Figure 3(b).



(a)

(b)

Figure 3:(a)Geometry for calculating the maximum forming angle (b) Measurement of strain on 3d microscope

To determine the minimum thickness, the formed sample was dissected from its center, and measurements were taken near the necking area using a digital micrometer. Additionally, surface roughness analysis was conducted on the interior of the produced component. The surface roughness at specific locations was assessed utilizing a Mitutoyo SJ-400. This approach enabled precise evaluation of both thickness variation and surface texture, contributing to a comprehensive understanding of the formed component's quality and characteristics.

III. Result and Discussion:

The selected process parameter combinations utilized for the experiment, along with the response parameters, were tabulated in Table 2. The process parameters considered were step depth, forming speed, and spindle speed, while the response parameters included maximum forming wall angle, minimum thickness, and roughness. In order to gain an overall understanding of the forming behavior of the bimetallic sheet, the researchers also took into account a forming limit diagram.

The study demonstrated the influence of different process parameters on the Single Point Incremental Forming (SPIF) technique. It was determined that the most influential parameters were step depth, forming speed, and spindle rotational speed. Through the conducted experiments, it was observed that setting the step depths below 0.2 mm led to folding and tearing of the material. Conversely, increasing the step depths beyond 1.0 mm resulted in significant shape deviation primarily caused by the spring-back effect. Figure 4 illustrates the tearing observed in the formed samples.

Table 2: Experimental plan with response parameters

Sr. No	Step Depth (mm)	Spindle Speed (rpm)	Forming Speed (mm/min)	Maximum Forming Wall Angle (Degree)	Minimum Thickness (mm)	Surface Roughness (μm)
1	0.1	1500	750	34.25	*	*
2	1.1	1500	750	52.23	0.6	
3	0.6	400	750	61.02	0.49	3.35
4	0.6	2600	750	62.32	0.41	1.91
5	0.6	1500	200	42.14	0.34	*
6	0.6	1500	1300	59.38	0.31	1.52
7	0.4 (Al-Cu)	2000	1000	65.35	0.53	1.42
8	0.4 (Cu-Al)	2000	1000	69.72	0.45	0.83

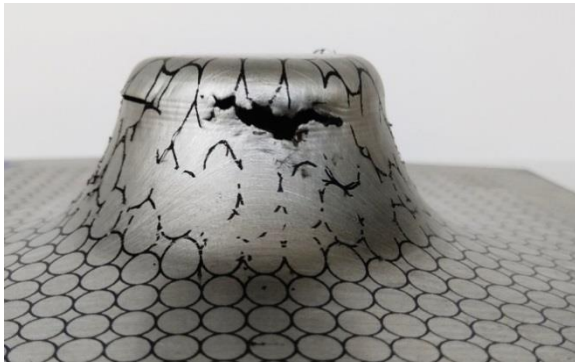


Figure 4: Tearing on Cu-Al arrangement and in Al-Cu arrangement

Forming speeds lower than 250 mm/min resulted in galling from adhesion between the tool and sheet material, whereas speeds surpassing 1250 mm/min caused material reduction. Degradation in surface quality was observed at tool rotation speed below 500 rpm, whereas tool rotation speed surpassing 2500 rpm caused minor vibration in the tool holding spindle. Moreover, spindle speeds lower than 500 rpm resulted in a decline in surface finish quality, whereas speeds exceeding 2500 rpm led to slight tool vibration during forming. Additionally, the accompanying figure illustrates the variations in thickness across different layer arrangements, providing a comprehensive insight into the effects of layer arrangement on the forming process.

Figure 5 illustrates material thinning in both Al-Cu and Cu-Al layer arrangements. The significant thinning observed suggests a potential risk of crack formation due to excessive thinning. The initiation of cracks appears to be closely linked to reaching the maximum angle for wall formation. It is noteworthy that the Cu-Al layer configuration displays a more uniform distribution of thickness, along with notably higher values for the maximum forming wall angle compared to the Al-Cu arrangement.

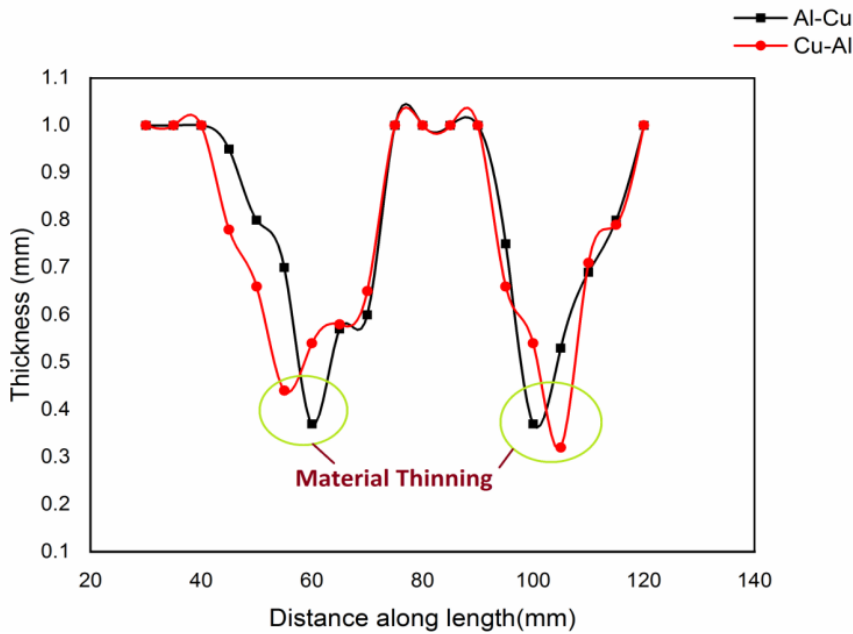


Figure 5: Thickness variations in layer arrangements

In the systematic analysis of the single-point incremental process conducted in this experimental study, the researchers examined the maximum forming wall angle and forming limit diagram. Figure 6 presents the forming limit curves for both the Al-Cu and Cu-Al layer configuration. It is apparent from the figure that the Cu-Al layer configuration allows for the attainment of maximum formability. Additionally, a forming wall angle of 69.72° was achieved in the Cu-Al layer arrangement, while 65.35° was achieved in the Al-Cu layer arrangement. The experimental results indicate a good agreement between the forming limit curve and the maximum forming wall angle for the conducted experiments.

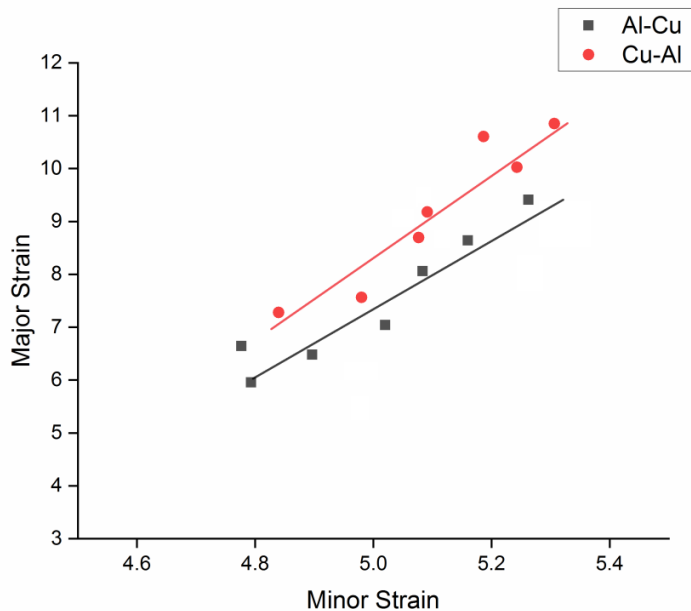


Figure 6: Forming limit diagram of successfully formed components

IV. Conclusion

In conclusion, the investigation conducted on Cu-Al composite sheet using SPIF, with consideration given to process parameters including step depth, forming speed, tool rotation speed, and layer configuration, has provided valuable insights. The following conclusions can be drawn:



- Step depths within the range of 0.2mm to 1.0 mm have been found to enhance forming depth, consequently improving the forming wall angle.
- Forming speeds ranging from 250 mm/min to 1250 mm/min contribute to improved thickness variation in the formed components.
- Spindle speeds falling between 500 rpm to 2500 rpm have been observed to enhance the surface finish of the formed components.

Furthermore, when compared to the Al-Cu layer arrangement, the Cu-Al layer arrangement has demonstrated a higher maximum angle for wall formation. Additionally, the forming limit diagrams of both layer arrangements exhibit good agreement with the results obtained for the maximum forming wall angle. These findings collectively contribute to a deeper understanding of the SPIF process and its optimization parameters for the Cu-Al bimetallic sheet.

References

- [1] Vahdani M, Mirnia M J, Gorji H and Bakhshi-Jooybari M 2019 Experimental Investigation of Formability and Surface Finish into Resistance Single-Point Incremental Forming of Ti-6Al-4V Titanium Alloy Using Taguchi Design *Trans. Indian Inst. Met.*
- [2] Sakhtemanian M R, Honarpisheh M and Amini S 2018 Numerical and experimental study on the layer arrangement in the incremental forming process of explosive-welded low-carbon steel/CP-titanium bimetal sheet *Int. J. Adv. Manuf. Technol.* **95** 3781–96
- [3] Behera A K, de Sousa R A, Ingarao G and Oleksik V 2017 Single point incremental forming: An assessment of the progress and technology trends from 2005 to 2015 *J. Manuf. Process.* **27** 37–62
- [4] Li Y, Chen X, Liu Z, Sun J, Li F, Li J and Zhao G 2017 A review on the recent development of incremental sheet-forming process *Int. J. Adv. Manuf. Technol.* **92** 2439–62
- [5] Hussain G, Gao L and Dar N U 2007 An experimental study on some formability evaluation methods in negative incremental forming **186** 45–53
- [6] Arfa H, Bahloul R and BelHadjSalah H 2013 Finite element modelling and experimental investigation of single point incremental forming process of aluminum sheets: Influence of process parameters on punch force monitoring and on mechanical and geometrical quality of parts *Int. J. Mater. Form.* **6** 483–510
- [7] Chezian Babu S and Senthil Kumar V S 2012 Experimental studies on incremental forming of stainless steel AISI 304 sheets *Proc. Inst. Mech. Eng. Part B J. Eng. Manuf.* **226** 1224–9
- [8] Ali M, Mirkouei A, Yu X, Malhotra R and Pilla S 2015 Journal of Materials Processing Technology Effects of incremental depth and tool rotation on failure modes and microstructural properties in Single Point Incremental Forming of polymers *J. Mater. Process. Tech.* **222** 287–300
- [9] Centeno G, Bagudanch I, Martínez-Donaire A J, García-Romeu M L and Vallellano C 2014 Critical analysis of necking and fracture limit strains and forming forces in single-point incremental forming *Mater. Des.* **63** 20–9
- [10] Silva M B, Bay N and Martins P A F 2015 *Hole-flanging by single point incremental forming* (Elsevier Ltd.)
- [11] Jeswiet J and Young D 2005 Forming limit diagrams for single-point incremental forming of aluminium sheet *Proceedings of the Institution of Mechanical Engineers, Part B: Journal of Engineering Manufacture* vol 219pp 359–64
- [12] Buffa G, Campanella D and Fratini L 2013 On the improvement of material formability in SPIF operation through tool stirring action *Int. J. Adv. Manuf. Technol.* **66** 1343–51
- [13] Silva M B, Skjoedt M, Martins P A F and Bay N 2008 Revisiting the fundamentals of single point incremental forming by means of membrane analysis *Int. J. Mach. Tools Manuf.* **48** 73–83
- [14] Li J, Hu J, Pan J and Geng P 2012 Thickness distribution and design of a multi-stage process for sheet metal incremental forming *Int. J. Adv. Manuf. Technol.* **62** 981–8
- [15] Li J C, Li C and Zhou T G 2012 Thickness distribution and mechanical property of sheet



metal incremental forming based on numerical simulation *Trans. Nonferrous Met. Soc. China (English Ed.* **22** s54–60

[16] Durante M, Formisano A and Langella A 2011 Observations on the influence of tool-sheet contact conditions on an incremental forming process *J. Mater. Eng. Perform.* **20** 941–6

[17] Bhattacharya A, Singh S, Maneesh K, Reddy N V and Cao J 2011 Formability and Surface Finish Studies in Single Point Incremental Forming *ASME 2011 Int. Manuf. Sci. Eng. Conf. Vol. 1* **133** 621–7

[18] Kotobi M, Mansouri H and Honarpisheh M 2019 Investigation of laser bending parameters on the residual stress and bending angle of St-Ti bimetal using FEM and neural network *Opt. Laser Technol.* **116** 265–75

[19] Afshin E and Kadkhodayan M 2015 An experimental investigation into the warm deep-drawing process on laminated sheets under various grain sizes *Mater. Des.* **87** 25–35